12th International Conference on Domain Decomposition Methods
Editors: Tony Chan, Takashi Kako, Hideo Kawarada, Olivier Pironneau,

12. Mortar Projection in Overlapping Composite Mesh Difference Methods

Serge Goossens[1], Xiao-Chuan Cai[2]

Introduction

We study experimentally the effect of the mortar projection in an overlapping composite mesh difference method for two-dimensional elliptic problems. In [CDS99], an overlapping mortar element method was proposed. This method has several desirable properties. For example, the discretisation is consistent, the accuracy is of optimal order and the error is independent of the size of the overlap, as well as the ratio of the mesh sizes. However, a major disadvantage of the method is that it needs weights in the bilinear form. The artificially introduced piecewise constant weights make the scheme consistent, but at the same time make it impossible to use fast solvers for the subdomain problems. On the other hand, the composite mesh difference method (CMDM) [Sta77, CMS00, GC99] does not need any weights, and its accuracy is also of optimal order if used with higher order interface interpolations. For example, the 2D bicubic or modified 1D cubic interface interpolation [GC99] is needed if one uses P1 or Q1 finite elements for the interior of the subdomains. But if the computationally more efficient low order interpolation is used on the interfaces, it may lead to a local inconsistent discretisation, resulting in an error that depends on the size of the overlap. The goal of this paper is to take the mortar approach, drop the weights and compare its results to the non-mortar methods. Of course, in an ideal scheme, which is yet to be discovered, the accuracy should be of optimal order and the error be independent of the size of the overlap and the ratio of mesh sizes. In order to be able to use fast solvers for the subdomain problems, it is also desirable not to have weights in the discretisation on the overlapping parts of subdomains.

Overlapping Nonmatching Grids Mortar Element Method

In this section we briefly describe the overlapping nonmatching grid mortar method. A two-subdomain version was given in [CDS99] and a many subdomain version was given by Maday et al[3]. Let $\Omega = \Omega_1' \cup \Omega_2'$ be the union of two overlapping, polygonal

[1]Department of Computer Science, K. U. Leuven, Celestijnenlaan 200A, B3001 Leuven, Belgium (`Serge.Goossens@cs.kuleuven.ac.be`, `http://www.cs.kuleuven.ac.be/~serge/`). Part of this work was carried out during the visit of the first author to the University of Colorado at Boulder. The financial support for this visit by the FWO-Vlaanderen is gratefully acknowledged. This research is financed by a specialisation scholarship of the Flemish Institute for the Promotion of Scientific and Technological Research in Industry (IWT).

[2]Department of Computer Science, University of Colorado at Boulder, Boulder, CO 80309-0430, USA (`cai@cs.colorado.edu`, `http://www.cs.colorado.edu/~cai/`).

[3]Presentation at the 12th International Conference on Domain Decomposition Methods, October 25–29, 1999, Chiba University, Chiba, Japan

subdomains. On each Ω_i' $(i = 1, 2)$, we define a function space for P1 or Q1 finite elements on a uniform grid with mesh size h_i and denote this function space by V_{h_i}. We denote $h = \min_i\{h_i\}$. We define the interface by $\gamma_i = \partial\Omega_i' \setminus \partial\Omega$ and the trace space $V_{h_i}(\gamma_j)$ as the restriction of V_{h_i} on γ_j. The mortar projection π_1 maps the space $V_{h_2}(\gamma_1)$ into $V_{h_1}(\gamma_1)$:

$$\int_{\gamma_1} (\varphi - \pi_1\varphi)\psi \; ds = 0 \;\; \forall\psi \in \tilde{\mathcal{W}}_{h_1}(\gamma_1). \tag{1}$$

The interface test function space $\tilde{\mathcal{W}}_{h_1}(\gamma_1)$ denotes the space of continuous piecewise linear functions that are constants in the first and last intervals, see [BMP94, CDS99]. Similarly we can define π_2. This projection is used in the definition of the solution space

$$V_h = \{(u_1, u_2) | u_1 \in V_{h_1}, u_2 \in V_{h_2}, u_{1|\gamma_1} = \pi_1(u_{2|\gamma_1}), u_{2|\gamma_2} = \pi_2(u_{1|\gamma_2})\}. \tag{2}$$

With the space V_h the variational form can be defined as:

$$\text{Find } u = (u_1, u_2) \in V_h \text{ such that } a_h(u, v) = f_h(v) \;\; \forall v = (v_1, v_2) \in V_h, \tag{3}$$

where the weighted bilinear form is defined as

$$\begin{aligned} a_h(u,v) &= \int_{\Omega_1'\setminus\Omega_2'} \nabla u_1.\nabla v_1 \; dx \; + \; \frac{1}{2}\int_{\Omega_1'\cap\Omega_2'} \nabla u_1.\nabla v_1 \; dx \\ &+ \frac{1}{2}\int_{\Omega_1'\cap\Omega_2'} \nabla u_2.\nabla v_2 \; dx \; + \int_{\Omega_2'\setminus\Omega_1'} \nabla u_2.\nabla v_2 \; dx \end{aligned} \tag{4}$$

and the right-hand side is given by

$$f_h(v) = \int_{\Omega_1'\setminus\Omega_2'} fv_1 \; dx \; + \; \frac{1}{2}\int_{\Omega_1'\cap\Omega_2'} fv_1 \; dx + \; \frac{1}{2}\int_{\Omega_1'\cap\Omega_2'} fv_2 \; dx \; + \int_{\Omega_2'\setminus\Omega_1'} fv_2 \; dx. \tag{5}$$

Here $f \in L^2(\Omega)$ is given. The theory by Cai et al. [CDS99] shows that the H^1 norm of the error is of order h. Their numerical results confirm this and show further that the L^∞ norm and the L^2 norm of the error are both of order h^2.

Composite Mesh Difference Method

A CMDM on two subdomains was described by Starius [Sta77], while Cai et al. [CMS00] studied the case of many subdomains. In [GC99] we outlined a CMDM for solving the second-order elliptic partial differential equation $\mathcal{L}u = f$ in Ω with a Dirichlet boundary condition $u = g$ on $\partial\Omega$.

Given a domain Ω consisting of p nonoverlapping subdomains Ω_i such that $\bar{\Omega} = \cup_{i=1}^{p}\bar{\Omega}_i$, we independently construct a grid of size h_i on each extended subdomain Ω_i' of Ω_i. Due to the extension of the subdomains these grids overlap. We denote by $\Gamma_i = \partial\Omega_i' \cap \partial\Omega$ the intersection of the boundaries $\partial\Omega_i'$ and $\partial\Omega$. The global discretisation $u_h = (u_{h_1}, u_{h_2}, \cdots, u_{h_p})$ on the composite grid is obtained by coupling the local discretisations through the requirement that the solution matches the interpolation

of the discrete solutions from adjacent grids. The system of equations consists of p subproblems, each having the following form:

$$\begin{cases} \mathcal{L}_{h_i} u_{h_i} = f_{h_i} & \text{in } \Omega_i', \\ u_{h_i} = g_{h_i} & \text{on } \Gamma_i, \\ u_{h_i} = z_{h_i} = \mathcal{I}_i u_h & \text{on } \partial\Omega_i' \setminus \Gamma_i. \end{cases} \tag{6}$$

Here $\mathcal{I}_i$ is an interface interpolation operator. As shown in [CMS00], the error in the discrete solution satisfies

$$\sum_{i=1}^{p} \|e_{h_i}\|_\infty \leq \left(1 + \frac{\sigma}{1-\tau}\right) \left(\sum_{i=1}^{p} K_i \|\alpha_i\|_\infty + \sum_{i=1}^{p} \|\beta_i\|_\infty\right). \tag{7}$$

In this bound the truncation error $\alpha_i(x) = (\mathcal{L}_{h_i} - \mathcal{L})\, u(x)$ is of order p_i:

$$\|\alpha_i\|_\infty \leq C_{\alpha_i} h_i^{p_i} \tag{8}$$

and the interpolation error $\beta_i(x) = (u - \mathcal{I}_i u)\,(x)$ is of order q_i:

$$\|\beta_i\|_\infty \leq C_{\beta_i} h_i^{q_i}. \tag{9}$$

The constants C_{α_i}, C_{β_i} and K_i are independent of the mesh size h_i. The interpolation constant $\sigma = \max_i \sigma_i$ is the maximum of the norms $\sigma_i = \|\mathcal{I}_i\|_\infty$ of the interpolation matrices. Let u_{h_i} be the solution of (6) with $f_{h_i} = 0$ and $g_{h_i} = 0$ restricted to the nonoverlapping domain $\bar{\Omega}_i$. Then, in terms of the data z_{h_i} on the interface $\partial\Omega_i' \setminus \Gamma_i$, it can be proved that

$$\|u_{h_i}\|_{\infty,\bar{\Omega}_i} \leq \rho_i \|z_{h_i}\|_{\infty,\partial\Omega_i' \setminus \Gamma_i}. \tag{10}$$

The convergence theory requires the contraction factor of the mapping to be smaller than 1, i.e. $\tau = \max_i (\rho_i \sigma) < 1$. Since ρ_i generally depends on the size of the overlap, τ may also depend on the size of the overlap.

Standard P1 Stencil & Bilinear Interpolation

Since both the standard P1 stencil and bilinear interpolation are second order, the error bound (7) shows that the resulting CMDM is also second order. However this scheme does not satisfy the consistent interpolation condition, see [GCR98, GC99], i.e.,

$$\frac{S}{h^2} - (u_{xx} + u_{yy}) = \frac{\gamma_k^2}{2} \left(\xi(1-\xi) u_{xx} + \eta(1-\eta) u_{yy}\right) + \mathcal{O}(h), \tag{11}$$

where S is the stencil, $\gamma_k = k/h$ is the ratio of the mesh sizes. The scaled local coordinates (ξ, η) used in the interpolation and the mesh sizes h and k are shown in Fig. 1. The scheme is consistent only if ξ and η are either 0 or 1, which implies that the two meshes match each other on the interface.

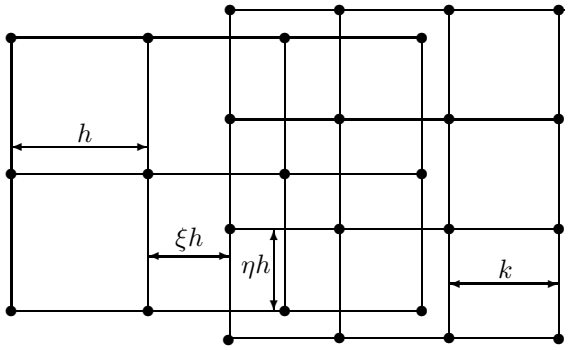

Figure 1: The scaled local coordinates (ξ, η) used in the interpolation.

Mortar Projection in CMDM

We now study a new scheme which takes the mortar approach and drops the weights in the bilinear form (4). In every subdomain we set up a finite element discretisation with the classic bilinear form

$$a_{h_i}(u_i, v_i) = \int_{\Omega_i} \nabla u_i . \nabla v_i \, dx \tag{12}$$

and use the mortar projection (1) to compute the Dirichlet conditions along the interfaces $\gamma_i = \partial\Omega_i' \setminus \Gamma_i$. Hence we have p local problems of the form (6). The mortar projection is a second order accurate interpolation and can be used in a CMDM. The interpolation constant σ can be larger than 1 in the bound $\|\pi\varphi\|_\infty \leq \sigma\|\varphi\|_\infty$ and we may need a large overlap to make the contraction factor ρ small enough in order to have $\tau < 1$.

In Fig. 2 we illustrate that the mortar projection does not, in general, satisfy the maximum principle, i.e. there exists a function φ that satisfies:

$$\|\pi\varphi\|_\infty > \|\varphi\|_\infty. \tag{13}$$

In this special example, the master function is obtained by sampling the function $\sin(\pi x)$ at the grid points $x_i^{(m)} = ih_m$ for $i = 0, 1, \ldots, 5$ where $h_m^{-1} = 5$. The slave nodes are $x_i^{(s)} = ih_s$ for $i = 0, 1, \ldots, 4$ where $h_s^{-1} = 4$. The slave function is set to 0 at the grid points $x_0^{(s)}$ and $x_4^{(s)}$ and the values at $x_i^{(s)}$ for $i = 1, 2, 3$ are determined from (1). We see that the slave function is larger than the master function at $x_2^{(s)} = 0.5$.

The P1 and Q1 finite element discretisations on a uniform mesh can be considered as finite difference stencils for which the local truncation error is second order. All the assumptions for a CMDM are satisfied and the error bound (7) shows that the resulting scheme is second order.

Due to the fact that the values for the Dirichlet boundary conditions on the interior subdomain boundaries, obtained by the mortar projection, are only $\mathcal{O}(h^2)$ accurate, the discretisations which use these values will be inconsistent, since the discretisation error contains the interpolation error divided by h^2. This leaves a constant term in

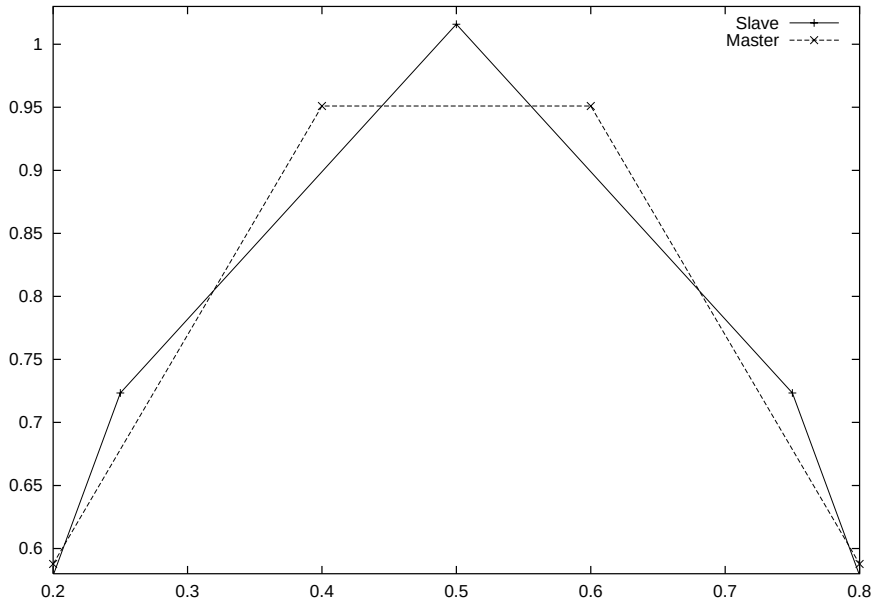

Figure 2: The mortar projection does not satisfy the maximum principle.

the error expansion of the combined discretisation interpolation pair, which does not tend to zero as the mesh size h tends to zero. Consequently this scheme does not satisfy the consistent interpolation condition defined in [GCR98] and we expect the global accuracy to depend on the size of the overlap.

The interpolation from the master to the slave side of the mortar on the interface is only one part of the interpolation issue. In the case of overlapping nonmatching grids we also need to compute the master side of the mortar, which requires evaluating the P1 or Q1 finite element function. This boils down to linear interpolation. As a result for P1 and Q1 finite elements a linear interpolation is done in the direction normal on interface.

Based on our experience with bilinear interpolation we can estimate the effect of doing linear interpolation in the direction normal on interface. Suppose the interface is at $x = x_\Gamma$ between the grid lines at x_i and x_{i+1}. The coefficients for the linear interpolation in the direction normal on the interface are $\xi = (x_\Gamma - x_i)/(x_{i+1} - x_i)$ and $(1 - \xi)$. We expect this interpolation to give rise to a term $\xi(1 - \xi)u_{xx}$ in the bound on the error in the extended subdomain just as in the case of the standard P1 stencil with bilinear interpolation. The numerical results in Table 1 clearly show the influence of the term $\xi(1 - \xi)u_{xx}$ in the error bound.

A final point is the dependency on the overlap. We have already pointed out that a large overlap may be required since the mortar projection does not satisfy the maximum principle. However this does not imply that the error on the nonoverlapping subdomain depends on the size of the overlap. The standard stencils with bicubic interpolation and our modified stencil with 1D cubic interpolation also require some

Table 1: Effect of inconsistent discretisation: results for P1 stencil with bilinear interpolation (columns 3–6) and with mortar projection (columns 7–10).

		bilinear interpolation				mortar projection			
l	ξ_1	$\|e_{\Omega'_1}\|_\infty$	γ_e	$\|e_{\Omega'_2}\|_\infty$	γ_e	$\|e_{\Omega'_1}\|_\infty$	γ_e	$\|e_{\Omega'_2}\|_\infty$	γ_e
0	0.6	1.65e-2		1.02e-2		2.95e-2		1.64e-2	
1	0.2	2.97e-3	5.57	2.98e-3	3.42	5.02e-3	5.88	5.02e-3	3.26
2	0.4	9.58e-4	3.10	1.55e-4	19.1	1.85e-3	2.71	1.57e-4	32.0
3	0.8	1.60e-4	6.00	2.59e-5	6.00	3.11e-4	5.96	2.59e-5	6.04
4	0.6	5.98e-5	2.67	9.70e-6	2.67	1.17e-4	2.66	9.71e-6	2.67
5	0.2	9.97e-6	6.00	1.62e-6	6.00	1.95e-5	5.99	1.62e-6	6.00
6	0.4	3.74e-6	2.67	6.06e-7	2.67	7.32e-6	2.66	6.06e-7	2.67

overlap in order to make sure that $\tau < 1$ because the interpolation constants are larger than 1. But the numerical results show that there is no dependency on the amount of overlap since these schemes are fully consistent.

In this case the error depends on the size of the overlap and this is due to the inconsistency mentioned above. In Table 2 we show numerical results illustrating the effect of the size of the overlap. These results also confirm the well known fact that increasing the size of the overlap results in faster convergence of the additive Schwarz method.

Numerical results

Our testcase concerns the solution of $-\nabla^2 u = f$ on $\Omega = \Omega_1 \cup \Omega_2$, where $\Omega_1 = [0,1]\times[0,1]$ and $\Omega_2 = [1,2]\times[0,1]$. The r.h.s. f and the Dirichlet boundary conditions g are chosen so that the exact solution is $u(x,y) = x^2$. The overlapping subdomains are $\Omega'_1 = [0, 1.4]\times[0,1]$ with $h_1 = 0.2\times 2^{-l}$ and $\Omega'_2 = [0.75, 2]\times[0,1]$ with $h_2 = 0.25\times 2^{-l}$.

In Table 1 we list the L^∞ norm of the error $\|e_{\Omega'_1}\|_\infty$ and $\|e_{\Omega'_2}\|_\infty$ on the overlapping extended domains Ω'_1 and Ω'_2 for the standard P1 stencil with bilinear interpolation and with mortar projection. Both these combinations satisfy all the assumptions for a CMDM so the error bound (7) shows that these methods are second order. For a second order scheme, the ratio between two successive error norms should be 4 when the mesh sizes are halved.

The discussion here is based on the bound on the error in every extended subdomain Ω'_i for the standard P1 stencil with bilinear interpolation. The presence of the inconsistency results in a dependency of the error on $\xi(1-\xi)$, i.e. the relative position of the interface in the other mesh. For this testcase the dominant term in the error bound is $e \approx (\xi(1-\xi)c_1 + c_2)\, h^2$, where c_1 and c_2 are constants independent of ξ and h. With this expression, we can estimate the ratio γ_e between two successive error norms. When the mesh is refined by halving the mesh size, i.e. $h_{i+1} = h_i/2$, we have

$$\gamma_e = \frac{\|e_{\Omega'_{h_i}}\|_\infty}{\|e_{\Omega'_{h_{i+1}}}\|_\infty} = \frac{c_1\,(\xi_i(1-\xi_i)+\gamma_c)\,h_i^2}{c_1\,(\xi_{i+1}(1-\xi_{i+1})+\gamma_c)\,h_{i+1}^2} = \frac{\xi_i(1-\xi_i)+\gamma_c}{\xi_{i+1}(1-\xi_{i+1})+\gamma_c}\,4 \qquad (14)$$

where $\gamma_c = c_2/c_1$. The worst case scenario is $\gamma_c = 0$ which results in values of 6.00

Table 2: Effect of overlap on the convergence rate of the Schwarz method and on the accuracy for the standard P1 stencil with mortar projection. The same results are obtained with bilinear interpolation.

m	$n_{\texttt{solver}}$	$n_{\texttt{prec}}$	$\|e_{\Omega_1}\|_\infty$	$\|e_{\Omega_2}\|_\infty$
0	587	35	1.00e-4	9.99e-5
1	305	26	4.42e-5	4.47e-5
2	159	19	1.74e-5	1.59e-5
3	83	14	6.01e-6	5.07e-6
4	44	10	4.81e-6	3.41e-6
5	24	8	1.77e-6	8.49e-7
6	13	6	1.31e-6	2.77e-7
7	8	5	2.51e-7	1.04e-8

and 2.67 for γ_e since in this testcase the term $\xi(1-\xi)$ alternates between 0.24 and 0.16. For the function $u(x,y) = x^2$ we have $\gamma_c \approx 0$. The numerical results in Table 1 show ratios γ_e equal to 6.00 and 2.67, illustrating the effect of the inconsistency due to linear interpolation in the x-direction.

Apart from this phenomenon both schemes are second order, since fitting a power of the mesh size $\|e_{\Omega_1'}\|_\infty \approx \kappa h^\lambda$ yields $\lambda \approx 2$. The second order accuracy can also be seen when the mesh is refined twice, i.e. the mesh size is divided by 4, in this case $\xi(1-\xi)$ does not change and we get ratios between two successive error norms, which are very close to the theoretical value of 16.

A fully consistent scheme such as the standard P1 stencil with bicubic interpolation or the modified stencil with 1D cubic interpolation by Goossens and Cai [GC99], computes the exact solution up to machine precision for this testcase on any grid.

In order to see the effect of the overlap, we fix the mesh sizes to be $h_1^{-1} = 320$ and $h_2^{-1} = 256$ and vary the overlap according to $\delta_1 = 2 \times 2^m h_1$ and $\delta_2 = 2^m h_2$ for the values of m listed in Table 2. This table shows the number of additive Schwarz iterations required to satisfy the convergence criterion of $\|r_n\|_2 \leq 10^{-10}\|r_0\|_2$ and the L^∞ norm of the error in the nonoverlapping subdomains Ω_1 and Ω_2. First we list the number of iterations ($n_{\texttt{solver}}$) the method needs when it is used a solver, i.e. in a Richardson iteration, in this case the convergence rate is bounded by τ. We also list the number of iterations ($n_{\texttt{prec}}$) the method needs when it is used as a right preconditioner for GMRES. As expected the number of additive Schwarz iterations decreases in both cases, as the overlap increases. These results clearly show the advantage of using a Krylov subspace method to accelerate the convergence of the iterative solver. From the results it is clear that the global accuracy of these two methods increases as the overlap increases, thus necessitating substantial overlap. The sensitivity to the size of the overlap is quite high since the error decreases 3 orders of magnitude when the overlap is increased from $m = 0$ to $m = 7$. This is highly undesirable. With a consistent scheme, this error would be independent of the size of the overlap.

Concluding remarks

We studied the effect of using a mortar projection as the interface interpolation in a composite mesh difference method for overlapping nonmatching grids problems. In this case the results are comparable to using bilinear interpolation for the Dirichlet boundary conditions on the interfaces. This is due to the fact that a linear interpolation in the direction that is normal to the interface is used to define the values on the master side of the interface. This results in a dependency of the error on the relative position of the interface nodes in the other mesh. Also due to the inconsistency, the global accuracy depends on the size of the overlap.

References

[BMP94]Christine Bernardi, Yvon Maday, and Anthony T. Patera. A new non conforming approach to domain decomposition: The mortar element method. In Haim Brezis and Jacques-Louis Lions, editors, *Collège de France Seminar*. Pitman, 1994. This paper appeared as a technical report about five years earlier.

[CDS99]X.-C. Cai, M. Dryja, and M. V. Sarkis. Overlapping nonmatching grid mortar element methods for elliptic problems. *SIAM J. Numer. Anal.*, 36:581–606, 1999.

[CMS00]X.-C. Cai, T. P. Mathew, and M. V. Sarkis. Maximum norm analysis of overlapping nonmatching grid discretizations of elliptic equations. *SIAM J. Numer. Anal.*, 37:1709–1728, 2000.

[GC99]S. Goossens and X.-C. Cai. Lower dimensional interpolation in overlapping composite mesh difference methods. In C-H. Lai, P. Bjørstad, M. Cross, and O. Widlund, editors, *Eleventh International Conference on Domain Decomposition Methods*, pages 248–255, Bergen, Norway, 1999. Domain Decomposition Press.

[GCR98]S. Goossens, X.-C. Cai, and D. Roose. Overlapping nonmatching grids method: Some preliminary studies. In J. Mandel, C. Farhat, and X.-C. Cai, editors, *Domain Decomposition Methods 10*, pages 254–261, Providence, RI, 1998. AMS.

[Sta77]G. Starius. Composite mesh difference methods for elliptic boundary value problems. *Numer. Math.*, 28:243–258, 1977.